1958-06

The Diurnal Temperature Wave with a Coefficient of Diffusivity Which Varies Periodically with Time and Exponentially with Height

THE DIURNAL TEMPERATURE WAVE WITH A COEFFICIENT OF DIFFUSIVITY WHICH VARIES PERIODICALLY WITH TIME AND EXPONENTIALLY WITH HEIGHT

By G. J. Haltiner

U. S. Naval Postgraduate School

(Manuscript received 28 October 1957)

ABSTRACT

The partial differential equation for heat diffusion is numerically integrated by the Runge-Kutta method. Solutions are obtained for the diurnal temperature variation with a bounded coefficient of eddy diffusivity which varies periodically with time and exponentially with height. The surface wave is represented by the sum of a diurnal and a semidiurnal harmonic wave. The results may be interpreted to apply over a fairly broad range of diffusivity values and height. With appropriate choices of the various parameters, reasonably good agreement is obtained between theoretical and observational values of amplitude reduction and phase lag as functions of height and time.

1. Introduction

The process of heat diffusion is involved in many problems confronting meteorologists. In particular, the diurnal temperature cycle has received much attention. Sutton [7] has presented a comprehensive survey of the classical theory of daily temperature variation, while an article by Staley [6] includes a summary of the more recent contributions to the problem.

The Taylor heat-diffusion equation for the diurnal temperature wave may be written in the well-known form

$$\frac{\partial \theta}{\partial t} = \frac{\partial}{\partial z}\left(K\frac{\partial \theta}{\partial z}\right). \tag{1}$$

Here t represents the time; z, the height; and $\theta(z,t)$, the potential temperature deviation from a mean value. In general, the coefficient of eddy diffusivity K is a function of both height and time at any particular location. The associated boundary conditions are usually taken to be

$$\theta = 0 \quad \text{for} \quad z = \infty, \quad \text{and all } t; \tag{2}$$

$$\theta = \theta_0(t) \quad \text{for} \quad z = 0. \tag{3}$$

The function $\theta_0(t)$ is normally represented by a single trigonometric term; however, more general solutions, which retain an arbitrary $\theta_0(t)$, have been found for certain forms of K. Solutions for the system of equations (1), (2), and (3) have been obtained for diffusivity coefficients which vary (a) linearly with z [3]; (b) as a power of z [4], [1] and (c) as a bounded exponential function of z [6]. The most general form of diffusivity adopted thus far appears to be that used by Poppendiek [5], who obtained a solution for a K which varied linearly with height and sinusoidally with time. However, because of the complexity of the solution, Poppendiek gave no numerical results. Very recently, de Vries [1] presented a method of solution for the case in which the eddy diffusivity is represented by a different function of height in an arbitrary number of layers.

The purpose of this paper is to present a numerical solution for the system (1), (2), (3) for a quite general form of K, as well as a representative form for $\theta_0(t)$.

2. The heat diffusivity coefficient

From physical considerations, the heat diffusivity K may be expected to increase with height at low levels since very near the ground vertical mixing is inhibited by the adjacent boundary surface. On the other hand, we should not expect to have K increase indefinitely with height; hence, a bounded diffusivity coefficient, such as that used by Staley [6], would seem more suitable than simply a power of z.

With regard to the diurnal variation of the diffusivity, it appears reasonable to expect that K would more or less follow the surface temperature wave, reaching maximum and minimum values near the time when the temperature is maximum and minimum, respectively. Staley [6] has discussed the diurnal variation of the eddy diffusivity. He points out that Poppendiek and Lettau found a sinusoidal variation of this coefficient with time. On the other hand, observations at 0.75 m at the University of Washington, and at 15 and 35 m at Manor, Texas (see [6]), indicate a general nighttime minimum and a daytime maximum but a somewhat erratic behavior otherwise. During the daytime, the larger diffusivity produces a rapid response to temperature disturbances and thus tends to remove transient effects more rapidly than at nighttime. Now the introduction of a diurnal varia-

tion into the coefficient of eddy diffusivity introduces great complexity into the problem of obtaining an analytic solution to the boundary-value problem at hand. Hence, to avoid the "pyramiding complexity" involved in an eddy diffusivity which varied with time, Staley chose a diffusivity coefficient characteristic of daytime values (including a height variation) for application to the time of maximum temperature.

The analytical difficulties mentioned above are largely absent when a numerical solution is sought except, perhaps, in connection with a study of computational stability or round-off error. It is essentially no more difficult to provide a solution to the boundary-value problem when there is a diurnal variation to the coefficient of eddy diffusivity. In connection with the observations of eddy diffusivity, some erratic variations of magnitude might be expected as a result of fluctuations of wind velocity, surface heating, turbulence, *etc.* If some are smoothed, the observations of eddy diffusivity can be well approximated by a finite trigonometric series; if not, by a single sine term. For the purposes of this investigation, two trigonometric terms were used; however, additional harmonics may be added at will.

Staley has suggested that a step-function for the time variation of K would be of interest. However, such time discontinuities in diffusivity do not appear to be justified. It should be mentioned, however, that such a solution can easily be treated essentially as a special case of the solution given below.

Temperature data indicate that, in general, the surface diurnal temperature wave can be well approximated by two trigonometric terms. It being assumed now that the eddy diffusivity follows the temperature wave, the following forms were assumed for $\theta_0(t)$ and $K(z, t)$.:

$$\theta_0 = a_4(\sin \omega t + c \sin 2\omega t) \tag{4}$$

$$K = g(t)a_1[1 - a_2 \exp(- a_3 z)], \tag{5}$$

where

$$\omega = 2\pi/86{,}400 \text{ sec}^{-1},$$

and

$$g(t) = 1 + b(\sin \omega t + c \sin 2\omega t). \tag{6}$$

The quantities a_1, a_2, a_3, a_4, b, and c are constants, appropriate values of which will be assigned later.

3. A transformation of coordinates

It will now be advantageous to place the basic equations into a form which will give a broader interpretation of the results. Assume that all quantities in the system of equations (1), (2), and (3) are expressed in c.g.s. units; then let

$$z = 100q\sigma, \quad t = 3600\tau. \tag{7}$$

Here q is a constant, while σ and τ are the new variables. With t in seconds, the units of τ are hours. For z in cm, σ will be in units of "q-meters"; *i.e.*, in 1-m units when $q = 1$, in 2-m units when $q = 2$, *etc.* With the transformation (7), (1) and (5) become

$$\frac{\partial \theta}{\partial \tau} = \frac{0.36}{q^2} \frac{\partial}{\partial \sigma} \left(K \frac{\partial \theta}{\partial \sigma} \right) \tag{8}$$

$$K = g(\tau)a_1[1 - a_2 \exp(- \alpha\sigma)], \tag{9}$$

where $\alpha = 100qa_3$. The forms of $g(\tau)$ and $\theta(\tau)$ remain the same as given by (4) and (6) except that ω must now be taken as $2\pi/24$. Similarly, the boundary conditions, (2) and (3), remain identical in form.

4. Finite difference equations

In order to obtain a numerical solution of the problem, we shall replace the derivatives of θ in (8) with appropriate finite difference forms. The problem is then reduced to one of solving a system of linear algebraic equations in the values of θ over a grid of points covering the desired range of time and height.

Expressing the derivatives of θ with respect to σ in (8) as finite difference ratios leads at once to the result

$$\frac{d\theta_i}{d\tau} = \frac{0.36}{q^2} \left[\left(\frac{dK}{d\sigma} \right)_i \frac{\theta_{i+1} - \theta_{i-1}}{2h} + K_i \frac{\theta_{i+1} - 2\theta_i + \theta_{i-1}}{h^2} \right]. \tag{10}$$

Here the subscript i designates the i'th level of the vertical grid at height ih, where h is the vertical distance between the points of the grid in units of σ, that is, q-m. The system of equations represented by (10) may be expressed in symbolic form as

$$\frac{d\theta_i}{d\tau} = A_i\theta_{i+1} + B_i\theta_{i-1} - C_i\theta_i, \tag{11}$$

$$A_i = \frac{0.36}{q^2} \left[\frac{1}{h^2} K_i + \frac{1}{2h} \left(\frac{dK}{d\sigma} \right)_i \right]$$

$$B_i = \frac{0.36}{q^2} \left[\frac{1}{h^2} K_i - \frac{1}{2h} \left(\frac{dK}{d\sigma} \right)_i \right] \tag{12}$$

$$C_i = A_i + B_i, \quad i = 1, 2, \cdots n.$$

The partial differential equation (1) has now been reduced to a system of ordinary differential equations which will be integrated numerically by the Runge-Kutta method [2].

5. A second transformation of coordinates

Observation and theory indicate that the most pronounced variations of temperature take place near the earth's surface. Thus a relatively small vertical grid distance is desirable at low levels, while at higher elevations a small grid distance is not necessarily needed. This suggests that a further transformation of

the vertical coordinate, so as to provide greater resolution at low levels, may be useful. This may be accomplished by the transformation

$$s = \ln \sigma. \tag{13}$$

For this case, the lower boundary condition (3) may apply at a height of q meters, corresponding to $\sigma = 1$. With the transformation [13], (8) may be written as

$$\frac{\partial \theta}{\partial \tau} = \frac{0.36}{q^2} e^{-2s}\left[K\frac{\partial^2\theta}{\partial s^2} + \left(\frac{\partial K}{\partial s} - K\right)\frac{\partial \theta}{\partial s}\right]. \tag{14}$$

The derivatives with respect to s may be expressed as finite difference ratios over a finite increment $\Delta s = l$, again leading to a system of equations of the form (11), with A_i and B_i now given by

$$\begin{aligned} \frac{A_i}{B_i} &= [1 + b(\sin \omega\tau + c \sin 2\omega\tau)] \\ &\quad \times \frac{0.36a_1}{q^2}\frac{e^{-2s}}{l^2}\{[1 - a_2 \exp(-\alpha e^s)] \\ &\quad \pm [\alpha a_2 e^s \exp(-\alpha e^s) - 1 + a_2 \exp(-\alpha e^s)]\} \\ C_i &= A_i + B_i, \quad i = 1, 2, \cdots n. \end{aligned} \tag{15}$$

Numerical solutions of the system (11), subject to the boundary conditions, were obtained for both the linear and logarithmic vertical coordinates.

6. The constants

Logarithmic Case.—Next, appropriate values of l, h, n and $\Delta\tau$, as well as the constants a_1, a_2, *etc.*, will be chosen. Consider first the form with $\ln \sigma$ as the vertical coordinate. With a choice of $l = \ln 2$, and the lower boundary condition assumed to apply at a height of q-m, the i'th equation of the system (11) and (15) applies at the height $2^i q$-m. Thus successive values of i, beginning with the lower boundary condition, apply to the levels, 1, 2, 4, 8, 16, 32, 64, 128, 256, 528, *etc.* q-m. A fairly detailed picture of the vertical structure may be obtained if the upper-boundary condition (2) is assumed to apply at the height of 528 q-m. Of course, additional levels are easily added; however, the time required for numerical integration is proportionately increased. For the above choice, $\theta_9 \equiv 0$, and the system (11) to be solved consists of eight simultaneous ordinary differential equations together with (4) for θ_0. A numerical solution of this system was then obtained by the Runge-Kutta method on a National Cash Register 102A electronic computer. The choice of the appropriate time interval over which the integration was to be carried out depended intimately upon the size of the eddy diffusivity. As the latter increased, $\Delta\tau$ had to be decreased in order to maintain computational stability and reasonable accuracy.

As for some of the other constants, the following numerical values were selected as being representative

$$\begin{aligned} a_2 &= 0.9 & b &= 0.8 \\ \alpha &= 0.05 & c &= 0.3. \\ a_4 &= 0.5(^\circ\text{C}) \end{aligned} \tag{16}$$

The choice of a_2 gives a 10-fold variation of K with height. This variation will take place mainly in the first 75 q-m because of the choice of α; *i.e.*, in 75 m for $q = 1$, 150 m for $q = 2$, *etc.* Values of a_2 of 0.95 and 0.99 would give a 20-fold and 100-fold variation of K with height, respectively. On the other hand, the constants b and c give rise to a 21-fold diurnal variation of K with time.

This variation of K with height and time is roughly the order of magnitude indicated by observations taken at the University of Washington [6]. However, these observations did show a greater variation of K with height in the daytime than at night, and also a diurnal variation of K which increased with height[1].

In order to keep the integration time-interval from being prohibitively short, the value of a_1 was kept comparatively small. Numerical results in the logarithmic case were obtained for two values of a_1:

$$a_1 = 0.222 \times 10^3\ q^2\ \text{cm}^2\ \text{sec}^{-1},$$
$$a_1 = 0.278 \times 10^2\ q^2\ \text{cm}^2\ \text{sec}^{-1}.$$

The first of these values gives the following range for the coefficient of eddy diffusivity (5) in units of $\text{cm}^2\ \text{sec}^{-1}$:

$$\begin{aligned} &\text{At surface,} \quad K_{\max} = 0.424 \times 10^2 q^2, \quad K_{\min} = 2.0\, q^2. \\ &\text{At 75 } q\text{-m,} \quad K_{\max} = 0.424 \times 10^3 q^2, \quad K_{\min} = 20.0\, q^2. \end{aligned} \tag{17}$$

For $q \leqq 1$, these values of K are somewhat small for typical atmospheric conditions, except perhaps for cases of very slight turbulence. This is reflected in the results by a large phase lag and large amplitude reduction with increasing height. Nevertheless, such values of eddy conductivity are not unrealistic for the sea.

Larger values of q will provide coefficients of diffusivity which are appropriate for normal atmosphere conditions. However, note that since α is a function of q, the vertical distance over which the major increase of eddy diffusivity occurs is 75 q-m. Thus for the larger values of q, the vertical increase of K will be more gradual.

It should also be pointed out here that as q increases,

[1] It is possible to obtain a greater variation of the eddy diffusivity with height during the day than at night by making the quantities a_2 and a_3 vary with time. For example, we may define a_2 as

$$a_2 = a_2' + a_3''(\sin \omega t + 0.3 \sin 2\omega t).$$

Then a choice of $a_2' = 0.95$ and $a_3'' = 0.0352$ will yield a 100-fold variation of diffusivity with height at the time of maximum surface temperature, and a 10-fold variation with height at the time of minimum temperature.

the finite vertical distance over which the derivatives are evaluated also increases. In general, this implies that the accuracy of the finite-difference approximation will decrease with increasing q. This is particularly true very near the ground where the most rapid variation of temperature with height and time occurs. In this connection, it may be noted that the lower boundary condition may be taken to apply at some arbitrary lower level, not necessarily the earth's surface. Thus, if desirable, the first several meters may be effectively omitted.

Linear Case.—A much larger value of a_1 was used in the numerical solution with the linear vertical coordinate, as represented by (11) and (12); namely,

$$a_1 = 0.71 \times 10^4\ q^2\ \text{cm}^2\ \text{sec}^{-1}.$$

This value increases the magnitudes of K in (17) by a factor of 32. The other constants a_2, a_3, a_4, b and c were kept the same. The vertical increment h for the linear case was taken to be 15 q-m. This requires a rather large number of equations in the system (11) in order to obtain some semblance of detail, together with a reasonable height at which to apply the upper-boundary condition. Applying the upper-boundary condition (2) at $\sigma = 285$ q-m, (285 q-m = 938 q-ft) and the lower-boundary condition (1) at the earth's surface leads to a system of 18 equations for the intermediate levels. This represents some compromise; since for $q = 1$, the upper boundary condition applies at the rather low height of 938 ft. On the other hand, taking $q = 2$, gives a more reasonable level (1876 ft) for the upper-boundary condition but gives a larger vertical finite difference increment of 30 m.

In both the logarithmic and linear cases θ was assumed to be initially zero at all levels. Naturally, these initial values are reflected in the results. However, as the integration proceeds through successive diurnal cycles, the effect of the initial conditions steadily decreases, more rapidly when the diffusivity is relatively large.

7. Results

Case 1.—The results of the integrations are given by figs. 1 through 10. Fig. 1 shows the logarithmic case with $\Delta\tau = 1/16$ for the larger a_1 giving the range of diffusivity coefficient represented by (17). Values of θ are given relative to the lower-boundary amplitude, and the time scale approximately corresponds to local time in hours. Only the curves for θ_0 (at q-m) and the 2, 4, 6, 8, 32 and 64 q-m levels are shown. At the 128 and 256 q-m levels the potential temperature disturbance, though very small, was still increasing after 60 hr because of the relatively low rate of heat diffusion. Eventually, of course, these θ's would oscillate. Even at the lower levels the mean value of θ was slightly positive showing the effect of the initial values and the diurnal variation of diffusivity. Fig. 2 shows the relative amplitude as a function of height for the three successive maxima over the 60-hr period for which results were computed. Note that differences between successive maxima decrease with increasing time, as the effect of the initial values gradually diminishes. The amplitude reduction for the last minimum is also included and shows a greater reduction than the maximum θ, corresponding to the lower nocturnal diffusivity.

Fig. 3 shows the time lag in hours as a function of height for last maximum and minimum of fig. 1. Up through the 32 q-m level there is a greater lag in the minimum than in the maximum, which may be expected because of the larger diffusion coefficient prevailing during the day. At the 64 q-m level, how-

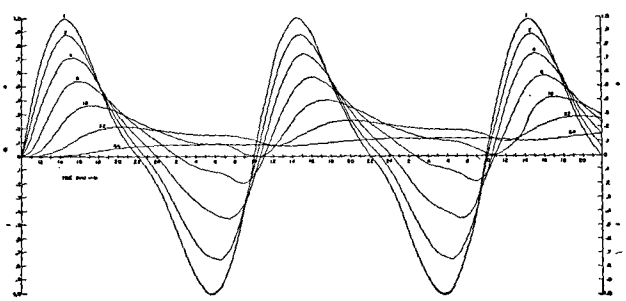

FIG. 1. Curves of θ, relative to the amplitude at the lower boundary, as a function of τ (in hours) at the 1, 2, 4, 8, 16, 32 and 64 q-m levels for $a_1 = .222 \times 10^3\ q^2\ \text{cm}^2\ \text{sec}^{-1}$.

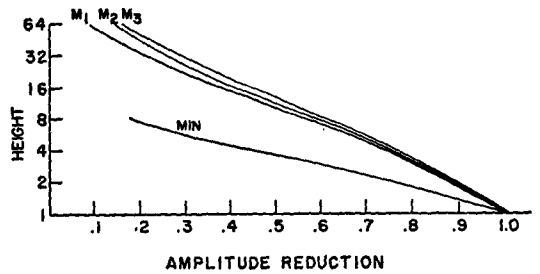

FIG. 2. Amplitude reduction as a function of height (in q-m) for the successive maxima M_1, M_2, M_3 and the last minimum of fig. 1.

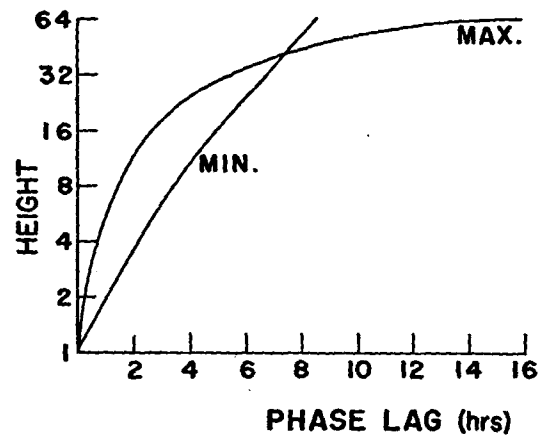

FIG. 3. Phase lag (in hours) as a function of height (in q-m) of the last maximum and minimum of fig. 1.

ever, there is a greater lag in the maximum than in the minimum. This may be explained by the relatively small mean diffusivity which gives rise to a minimum θ at the 64 q-m level at a time when the coefficient of diffusivity has reached a near maximum diurnally, thus decreasing the lag. Similarly, the maximum θ at 64 q-m occurs at a time when the coefficient of diffusivity is near a diurnal minimum.

Case 2.—In order to show more clearly the effect of the diurnal variation of the eddy diffusivity, a 40-hr run (fig. 4) was made with the constant, $b = 0$, thus eliminating the time variation of K. All other constants are the same as in Case 1. Fig. 5 shows the amplitude reduction of the two successive maxima, and the phase lag as a function of height is shown in fig. 6. The small differences between the curves of each figure are due primarily to the initial conditions since there is no time variation of the coefficient of diffusivity.

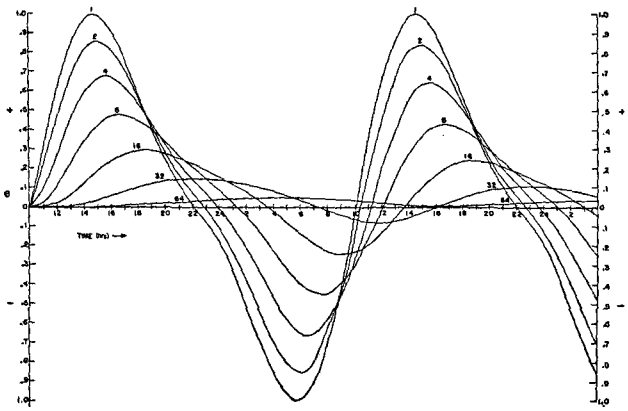

FIG. 4. Similar to fig. 1 except that $b = 0$; *i.e.*, the eddy diffusivity is a function of height only.

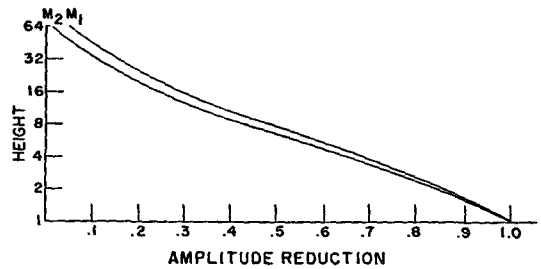

FIG. 5. Amplitude reduction for the two successive maxima of fig. 4.

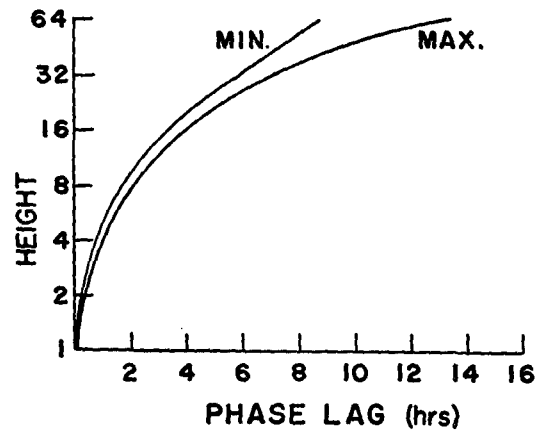

FIG. 6. Phase lag of the second maximum and the minimum of fig. 4.

Case 3.—Figs. 7 and 8 give the amplitude reduction and phase lag in the logarithmic case for the smaller value of a_1, corresponding to a smaller diffusivity than in Case 1. As would be expected, the amplitude reduction and phase lag are greater, level for level, than in Case 1.

Case 4.—Figs. 9 and 10 give the amplitude reduction and phase lag as functions of height, in the linear form (11 and 12) for a 24-hr run with $\Delta\tau = 1/64$. The curves for θ at the 18 intermediate levels are not presented since they are similar in general appearance to the curves of fig. 1. Of course, the phase lag and

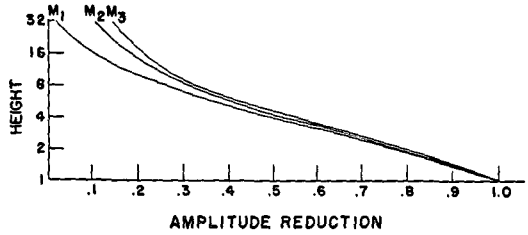

FIG. 7. Similar to fig. 2 for $a_1 = 0.278 \times 10^2\ q^2\ \text{cm}^2\ \text{sec}^{-1}$.

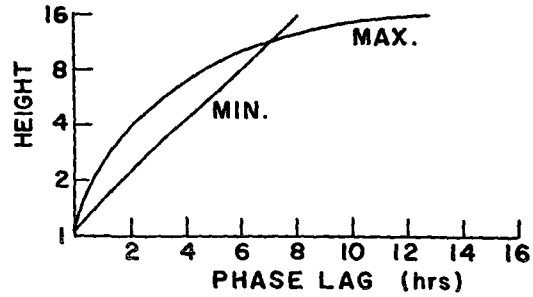

FIG. 8. Similar to fig. 3 for $a_1 = 0.278 \times 10^2\ q^2\ \text{cm}^2\ \text{sec}^{-1}$.

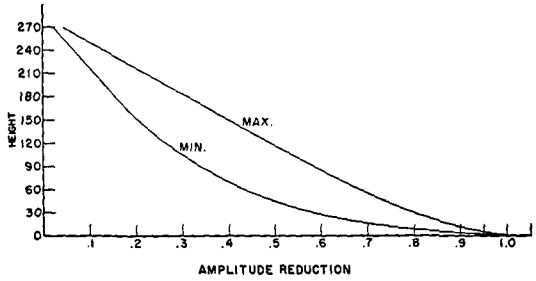

FIG. 9. Similar to fig. 2 for $a_1 = 0.71 \times 10^4\ q^2\ \text{cm}^2\ \text{sec}^{-1}$.

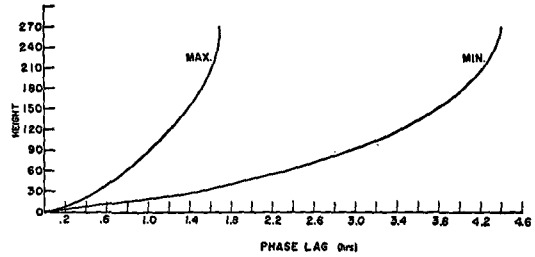

FIG. 10. Similar to fig. 3 for $a_1 = 0.71 \times 10^4\ q^2\ \text{cm}^2\ \text{sec}^{-1}$.

amplitude reduction differ considerably. The diffusion coefficient is much larger in this instance and the effects of initial conditions are correspondingly reduced. There is an appreciable difference between the amplitude reduction of the maximum and that of the minimum. For example, at 90 q-m, the maximum is about 58 per cent of the surface value of θ, while the minimum is only about 33 per cent of the surface minimum. At much lower and much higher levels, the difference between amplitude reduction of the maximum and minimum is less. The phase lag increases with altitude for both the maximum and minimum; but the rate of increase decreases with height because of the increase of the coefficient of diffusivity.

Some comparison between the various cases discussed above may be made by appropriate choices for q. The value, $q = 2.8$ in Case 3 gives the same range of diffusivity coefficients as $q = 1$ in Case 1; however, in the former the vertical increase of K is more gradual, and the finite vertical increment is increased by a factor of almost 3.

Similarly, a choice of $q = 5.65$ in Case 1 will give the same range of diffusivity as $q = 1$ in Case 4. Here again, the larger q gives a much more gradual increase of K with height, as well as a larger vertical finite difference increment. Thus the amplitude reduction and phase lag may be expected to differ somewhat even though the overall range of diffusivity is the same.

It should be remarked here that the computations were carried out to 9 decimal places in Cases 1, 2 and 3, and to 5 decimal places in Case 4. The scale of the graphical presentations is too small to show this detail; however, the data are too lengthy to present in numerical form. Some of the values given in the following section were read directly from the original data, rather than the graphs.

8. Comparison to some observations

It is of interest to compare the results obtained here to some actual data. Table 1 shows the relative amplitude[2] and phase lag from observations taken at the University of Washington (see [6]), together with results obtained from the numerical integration of Case 4 for $q = 2$. The agreement here is quite good; however, the height range is limited. Table 2 shows some observations taken for clear June days at Leafield (see page 220 [7]), which extend over greater heights. Theoretical values are taken again from Case 4 for $q = 2$. The amplitude reductions are expressed relative to the 10-m level. The agreement on amplitude reduction is again favorable; but the phase lags (see page 206 [7]) at Leafield are considerably larger than the theoretical values. A choice of $q = 6$ in Case 1, with the logarithmic vertical coordinate, gives somewhat better agreement with the data here. The phase lags for the 12, 30, 57, and 96 meter levels are 0.25, 1, 1.5, and 2.6 hr, respectively. However, the corresponding amplitude reductions are too large compared to the Leafield values. The phase lags for Ismailia [7] for clear days give fair agreement with Case 4, $q = 2$, as shown in table 3. It appears that even better results might be obtained here if $K \doteq 6 \times 10^3$ cm^2 sec^{-1} at the surface but increases more rapidly with height.

Table 4 compares the Eiffel Tower data (see [6])

TABLE 1. Amplitude reduction (A.R.) and phase lag (P.L.) taken from Case 4 for $q = 2$ *versus* observations at the University of Washington, Seattle.

Theory			Observation	
A.R.	P.L.	Height	A.R.	P.L.
0.92	13.5 min	15 meters	0.91	16 min
0.87	20	30	0.86	18
0.83	25.5	45	0.83	23
0.82	31	60	—	—

TABLE 2. Amplitude reduction (A.R.) and phase lag (P.L.) taken from Case 4, $q = 2$, *versus* observations taken at Leafield.

Theory			Leafield	
A.R.	P.L.	Height	A.R.	P.L.
—	—	12 meters	—	0.83 hr
—	—	25	0.90	—
0.90	20 min	30	—	1.20
—	—	50	0.84	—
0.82	31	60	—	1.5
0.76	40	90	—	1.66
—	—	100	0.77	—
0.71	—	120	—	—

TABLE 3. Phase lag for Case 4, $q = 2$ *versus* observations taken at Ismailia.

Theory	Height	Ismailia
14 min	16 meters	23 min
26	46	26
31	60	26

TABLE 4. Amplitude reduction from Eiffel Tower data *versus* theoretical values from Case 4, for $q = 2$ and $q = 3$.

Theory			Observations	
$q = 3$	$q = 2$	Height	Summer	Winter
0.89	0.825	195 meters	0.88	0.83
0.75	0.60	300	0.75	0.60

[2] The amplitude reductions given in tables 1, 2, and 4 denote the ratios of the upper maxima to the surface maximum for the various levels. If differences between upper maxima and minima are used to determine the amplitude reductions, the results are similar but require a somewhat larger value of q. For example, with $q = 2.5$, the amplitude reductions in table 1 are 0.91, 0.83, .78, and .74 and the phase lags are 11, 18, 23, and 23 minutes at the 15, 30, 45, and 60 meter levels, respectively. Similarly, in Table 4 a value of $q = 2.5$ gives amplitude reductions of 0.83 and 0.62 for the 195 and 300 meter levels, while the value $q = 4$ gives amplitude reductions of 0.87 and 0.73 at 195 and 300 meters, respectively. It should be noted here that, in accordance with equations 1 and 4, comparison of observation and theory, strictly speaking, should be based on deviations from the mean potential temperature at the lower boundary. However, the published data from Leafield, etc., was not available in this form.

with the Case 4 for $q = 2$ and $q = 3$. The theoretical amplitude reductions are expressed relative to the 120-m value. The data agree very well with the theory here. With regard to eddy diffusivity, the values $q = 2$ and $q = 3$ correspond to values of K which are 128 and 288 times the numbers in (17); namely,

q	z (meters)	K_{max} (cm^2 sec^{-1})
2	0	5.4×10^3
2	150	5.4×10^4
3	0	1.22×10^4
3	225	1.22×10^5

9. Summary and conclusions

A numerical solution has been presented for the diurnal temperature variation with a coefficient of eddy diffusivity which is a bounded function of height and a periodic function of time. By suitable selection of several parameters, reasonably good agreement has been obtained between theory and observation. The results emphasize that coefficient of eddy diffusivity varies seasonally and geographically, as do other meteorological parameters. No comparison was made to observations of minimum temperature; however, we may expect a diurnal variation of eddy diffusivity roughly similar to that assumed here.

It should be recalled that the functional form of K has been based mainly on reasonable physical grounds. A more desirable theory would be one in which the eddy diffusivity is linked to other meteorological variables, such as wind velocity, surface roughness, stability, *etc.* Note, however, that the coefficient of diffusivity assumed here does follow the surface temperature cycle and is thus related to the lapse rate and stability.

The author would like to express his thanks to Professor H. M. Martinez of the U. S. Naval Postgraduate School for his advice and assistance in programming this problem for the electronic computer.

REFERENCES

1. deVries, D. A., 1957: On the integration of the heat-conduction equation with periodic variation of temperature. *J. Meteor.*, **14**, 71–76.
2. Gill, S., 1951: A process for the step integration of differential equations in an automatic digital computing machine. *The Cambridge Phil. Soc. Meetings*, **47**, 96–108.
3. Haurwitz, B., 1936: The daily temperature period for a linear variation of the Austausch coefficient. *Trans. r. Soc. Canada*, 3rd Ser., **30**, 1–8.
4. Kohler, H., 1932: Ein kurzes Studium des Austausches auf Grund des Polenz gesetzes. *Beitr. Phys. fr. Atmos.*, **19**, 91–104.
5. Poppendiek, H., 1952: A periodic heat transfer analysis for an atmosphere in which the eddy diffusivity varies sinusoidally with time and linearly with height. *J. Meteor.*, **9**, 368–370.
6. Staley, D. O., 1956: The diurnal temperatures wave for bounded eddy conductivity. *J. Meteor.*, **13**, 13–20.
7. Sutton, O. G., 1953: Micrometeorology. New York, McGraw-Hill, 333 pp.